International Journal of Fracture **45**: 263–282, 1990.

A hybridized displacement discontinuity and indirect boundary element method to model fracture propagation

H.C.M. CHAN, V. LI and H.H. EINSTEIN
Department of Civil Engineering, Massachusetts Institute of Technology, Cambridge, MA 02139, USA

Received 1 June 1988; accepted in revised form 23 June 1989

Abstract. In mechanical modelling of fracture propagation, complications arise from the stress concentrations at the fracture tips and nonlinear responses caused by opening/closing of fractures, by nonlinear constitutive relations of fracture surfaces sliding on each other, and by fracture propagation. The hybridized Displacement Discontinuity and Indirect Boundary Element Method described in this paper avoids problems associated with other numerical methods when analyzing fracture propagation. The method, which includes analytical influence functions and thus makes numerical integration unnecessary, is described in the first part of this paper. In the second part a number of examples are given in which a variety of fracture propagation problems in two dimensions are modelled with the hybridized method. These examples include classical problems in which tension is applied to cracked plates but also others where shearing is applied. Comparisons with solutions obtained by other authors are shown to be satisfactory.

1. Introduction

In mechanical modelling of fracture propagation, complications arise from the stress concentrations at the fracture tips and nonlinear responses (even if the intact medium itself is linear elastic) caused by the opening/closing of fractures, by nonlinear constitutive relations of the fracture surfaces sliding on each other, and by fracture propagation. Commonly available numerical methods to deal with such complications include the Finite Element Method [1], the Displacement Discontinuity Method [2, 3], and the Direct and Indirect Boundary Element Methods [2, 4], each of which has advantages and disadvantages.

In the finite element formulation, singular elements can be used to capture the stress singularities at the fracture tips. When fracture propagation is modelled, the changing fracture geometry requires the element mesh to be continuously modified [5]. Such remeshing at every propagation step renders the finite element method inefficient.

In the direct boundary element formulation based on the point-force fundamental solution, considerable difficulties arise since the displacement discontinuities across the fracture surfaces are not explicitly accounted for. One approach to tackle this problem is to partition the medium (which must be finite) into sub-regions [6]. However, this approach becomes inefficient when there are two or more cracks, or even for a single crack which propagates out-of-plane in mixed mode loading.

In the indirect boundary element (or fictitious stress) formulation, difficulties similar to that of the direct boundary element method arise because continuous displacements are implicitly assumed.

The displacement discontinuity method is particularly well suited to model fractures which have relative displacements across their surface (hence a displacement discontinuity results). In addition, it can also be used to model an ordinary boundary of a 2- or 3-dimensional body. However, as will be shown later, strong stress singularities at the ends of the displacement elements make it undesirable to model boundaries with finite and smoothly distributed applied loads.

The formulation of the displacement discontinuity method is identical to that of the fictitious stress method except that displacement discontinuities (or "fictitious cracks") are used instead of fictitious stresses. (Naturally, the fundamental solution will also be different.) Hybridizing these two methods so that the advantages of both can be utilized seems to be very promising. In addition, the boundary element methods have further advantages over the finite element method when some special types of boundaries are present. For example, for a semi-infinite medium discretization of the traction-free surface of the medium is not necessary when the appropriate influence functions are incorporated. The same is true for an infinite or semi-infinite medium with a circular cavity.

In this paper a hybridized scheme using the displacement discontinuity and the indirect boundary element methods is presented. A two-dimensional, brittle, and linear elastic medium with fractures is modelled. The influence functions of the elements have been derived analytically, and numerical approximations are thus not required. Arbitrary geometries and loading sequences are possible. Generally, linear elastic fracture mechanics conditions are assumed. For closed fractures under shear, nonlinear stress-slip relations can be incorporated and for closed fracture tips under shear, a special element type can be optionally used. For geomechanical problems, geostatic stresses have been included for more realistic modelling. The computer program FROCK (acronym for Fractured ROCK) which incorporates all these features has been applied to various types of problems with or without fracture propagation. Some basic applications are presented in this paper to show that the chosen approach is satisfactory.

2. Basic formulation

A generalized problem of a two-dimensional, homogeneous and linear elastic medium with fractures and cavities can be represented as shown in Fig. 1. Usually the medium is bounded by a closed curve which is the external boundary. However, if the medium is large compared to the region of interest it may be considered infinite. Fractures and cavities, if any, are also regarded as part of the boundary.

As mentioned in the Introduction, the most expedient deformation analysis method for modelling crack problems in elastic media appears to be the displacement discontinuity method. Displacement discontinuity elements can be used to model fractures directly and efficiently. They can also be used to model the external boundaries (including cavities) but as will be shown in Section 4.1, there are considerable stress singularities near the displacement discontinuities. Thus hybridizing with another method which can better model external boundaries is desirable. The fictitious stress method, which is an indirect boundary element method, was selected for this purpose. In fact the displacement discontinuity method may also be viewed as an indirect boundary element method, except that the conventionally used fundamental solution of a line-force is replaced by that of a dislocation.

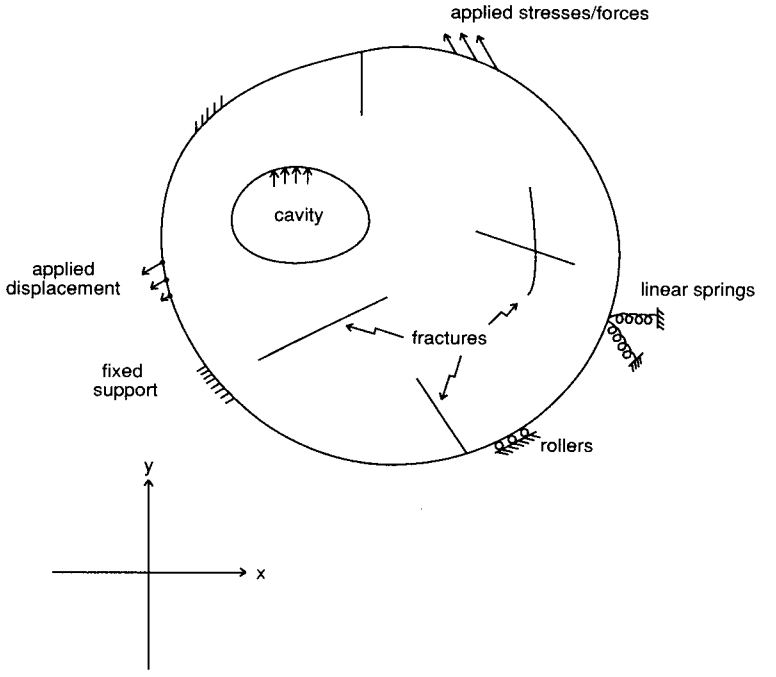

Fig. 1. A generalized plane problem.

In the hybridized indirect boundary element formulation, the stresses and strains in the medium are considered to be induced by a set of fictitious quantities instead of the applied loadings. The fictitious quantities act at the boundaries which are modelled by boundary elements. The justification is that if the fictitious quantities are distributed so as to induce the given conditions on the boundaries, then they can also induce the corresponding stresses and strains in the medium. This assertion follows directly from the uniqueness of solution for a linear problem with given boundary conditions [7]. Thus we have

$$\sigma(x, y) = \int_B (F_1(x, y; s)p_1 + F_2(x, y; s)p_2)\, \mathrm{d}s \ldots, \tag{1}$$

where σ is a component of the induced stresses at a point (x, y); p_1 and p_2 are the fictitious quantities in the shear (tangential to boundary) and normal (normal to boundary) senses respectively. F_1 and F_2 are respectively the induced stresses at (x, y) due to a unit applied shear and normal fictitious quantity at the position characterized by the coordinate s on the boundary B. F_1 and F_2 are called the fundamental solutions.

p_1 and p_2 can be applied tractions or distributed semi-infinite dislocations. For example, if p_2 represents an applied normal traction on the boundary (or a part of the boundary), F_2 represents Kelvin's solution [2] for a unit normal point force* at s. If p_1 represents an applied shear traction, F_1 represents Kelvin's solution for a unit shear point force at s. If p_2 is a distributed normal dislocation, then F_2 represents the induced stress due to a unit normal semi-infinite dislocation. In this case (p_2 ds) is equal to D_d of Fig. 2 which shows a shear and

* In 2-D analysis, a point force corresponds to a line force in 3-D.

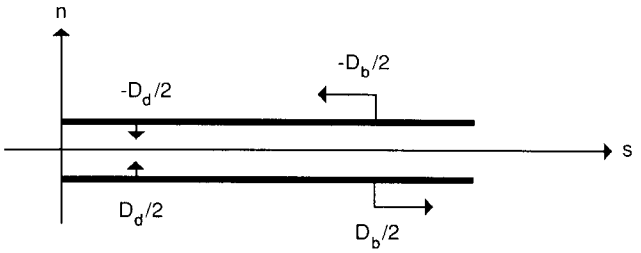

At point (s,n), induced (plane strain) stresses and displacements are given by (non-essential integration constants for the induced displacements are neglected):

$$\Delta\sigma_{ss} = CD_b\, n(3s^2+n^2)/r^4 + CD_d\, s(n^2-s^2)/r^4$$

$$\Delta\sigma_{sn} = -CD_b\, s(s^2-n^2)/r^4 + CD_d\, n(n^2-s^2)r^4$$

$$\Delta\sigma_{nn} = -CD_b\, n(s^2-n^2)/r^4 - CD_d\, s(3n^2+s^2)/r^4$$

$$u_s = \frac{D_d}{2\pi}\left[\frac{1-2\nu}{4(1-\nu)}\ln(s^2+n^2) - \frac{s^2-n^2}{4(1-\nu)(s^2+n^2)}\right] + \frac{D_b}{2\pi}\left[\text{atan}(n,s) - \pi + \frac{sn}{2(1-\nu)(s^2+n^2)}\right]$$

$$u = \frac{D_d}{2\pi}\left[\text{atan}(n,s) - \pi - \frac{sn}{2(1-\nu)(s^2+n^2)}\right] - \frac{D_b}{2\pi}\left[\frac{1-2}{4(1-\nu)}\ln(s^2+n^2) + \frac{s^2-n^2}{4(1-\nu)(s^2+n^2)}\right]$$

$$C = \frac{E}{4\pi(1-\nu^2)} \quad \text{and} \quad r^4 = (s^2+n^2)$$

where

atan (n,s) is the counterclockwise angle between the vector $\begin{bmatrix} s \\ n \end{bmatrix}$ and the positive s-axis and $0 < \text{atan}(n,s) < 2\pi$, $\text{atan}(0,s) = \pi$.

Fig. 2. A semi-infinite dislocation and its influence functions.

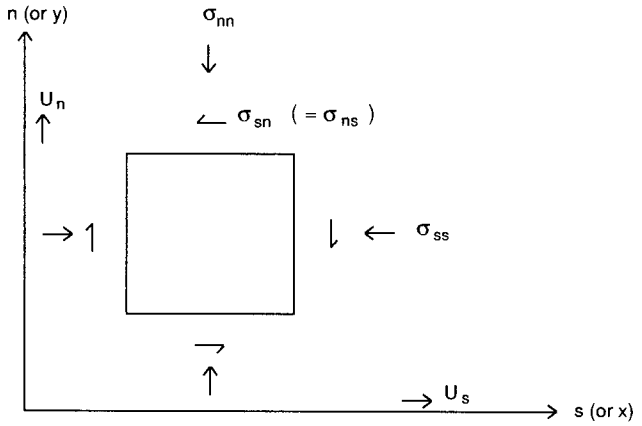

Fig. 3. Stress and displacement conventions.

a normal semi-infinite dislocation and lists the fundamental solutions for the induced stresses (Fig. 3 shows the sign conventions for stresses and displacements).

Similarly the induced displacements at (x, y) are given by

$$u(x, y) = \int_B [G_1(x, y; s)p_1 + G_2(x, y; s)p_2] \, ds \ldots, \tag{2}$$

where G_1 and G_2 are the fundamental solutions for the displacements.

In a problem where the external boundary is modelled by fictitious stress elements and the fractures are modelled by displacement discontinuity elements, the indirect boundary element method and the displacement discontinuity method are hybridized. Many cases involving both displacement discontinuity and fictitious stress elements have been considered in [8].

Once $p_1(s)$ and $p_2(s)$ have been solved for by satisfying the appropriate boundary conditions, the entire problem is solved because the induced stresses and displacements at any point in the medium can then be calculated based on these fictitious quantities.

2.1. Boundary discretization

The (internal and external) boundaries are discretized into elements so that the given boundary conditions can be modelled. An element consists of two parallel surfaces separated by an arbitrarily small distance (Fig. 4). The beginning of the element is at the origin of the local s–n coordinate system. In our approach, straight elements are used, and curved boundaries can be approximated by a series of straight elements. For example, the problem in Fig. 1 can be discretized into a boundary element mesh shown in Fig. 5.

The solution procedure is further simplified by assuming a certain distribution of fictitious quantities in each of the elements. The types of fictitious quantities (applied tractions or dislocations) together with specific spatial distributions give rise to different types of elements (Sections 2.1.1. and 2.1.2).

In this formulation the distributional form of the fictitious quantities is prescribed separately for each of the elements. Neighbouring elements may not have the same distributional forms of fictitious quantities and generally there is no continuity in the distributions of fictitious quantities across them. This means singularities in the form of infinite stresses exist at the element ends. Thus calculated stresses at or near the element ends may not be reliable, especially when finite stresses are known to exist. However, as shown in the examples in Section 4, the singularities only affect calculated results near the element axes, and the calculated stress intensity factors can still be satisfactorily accurate.

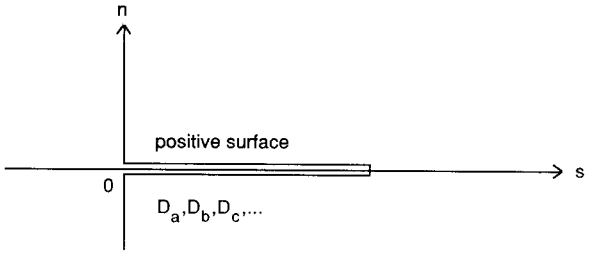

Fig. 4. An element with fundamental variables D_a, D_b, D_c . . .

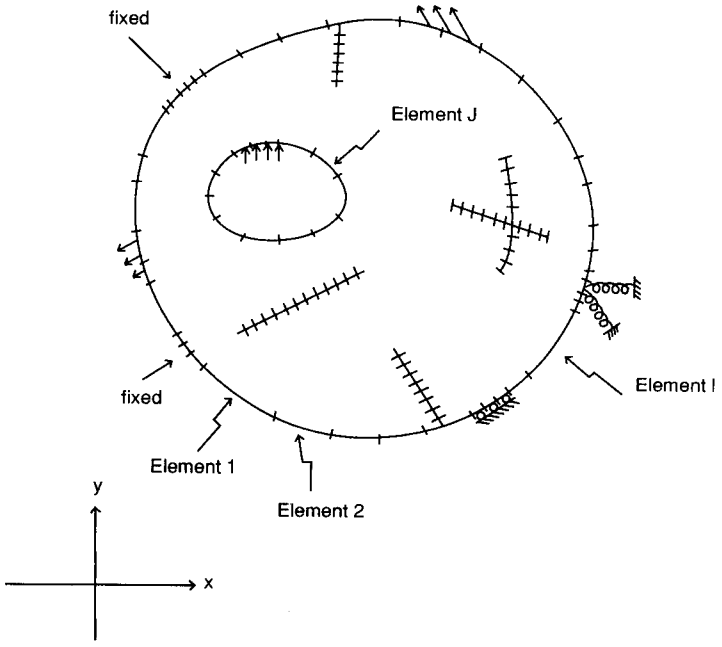

Fig. 5. Boundary discretization of the problem in Fig. 1.

This compatibility problem for neighbouring fracture elements in a straight fracture has been examined by Curran and Vandamme [3]. They tried both compatible and noncompatible elements in modelling the fracture. The noncompatible elements were found to give more accurate results, even though more degrees of freedom and computer time were required.

In cases with noncollinear neighbouring fracture elements this compatibility problem may be more serious. For example, [8] straight cracks with small kinks at the ends have been modelled. It was found that more elements were required to attain the same accuracy than in the case of entirely straight cracks.

In cases with intersecting cracks and surface cracks, such as the one seen in Fig. 5, usually better accuracy is obtained when the crack elements cross or intersect the other elements at their end points. In [8] the stress intensity factors of some star cracks were calculated using the numerical procedure. Better results were obtained when the intersection of the branches coincided with the end points of the crack elements. Also for more complicated crack geometry, such as a star crack with many branches, generally more elements must be used to maintain sufficient accuracy. In modelling surface cracks, such as the rock joint in a direct shear test and the surface crack in a compact tension test, satisfactory results were obtained when the crack elements intersect the surface elements at their end points. Generally speaking, even though intersecting elements are allowed in the numerical procedure, this problem has not been considered in full detail.

2.1.1. Stress discontinuity elements

A stress discontinuity element is one on which applied tractions act, resulting in a stress jump or discontinuity across the element axis [2]. In our approach the applied shear and normal

tractions p_1 and p_2 can either be uniformly or linearly distributed on the element axis. Thus

$$p_1 = p_s = [1 - s/(2a)]D_a + [s/(2a)]D_b \ldots, \tag{3}$$

$$p_2 = p_n = [1 - s/(2a)]D_c + [s/(2a)]D_d \ldots, \tag{4}$$

where D_a, D_b = shear tractions at beginning and end of element respectively; D_c, D_d = normal tractions at beginning and end of element respectively.

For a constant stress discontinuity element (CSDE) $D_a = D_b$ and $D_c = D_d$, while for a linear stress discontinuity element (LSDE) D_a to D_d are separate variables.

Thus by putting (3) and (4) into (1) and (2), D_a to D_d become the unknowns to be solved. These unknowns are called fundamental variables. The induced stresses/displacements of a fundamental variable are called its influence functions, which have been derived in closed form by Chan [8].

2.1.2. Displacement discontinuity elements

A displacement discontinuity refers to a displacement jump across the two surfaces of the element. A displacement jump occurs whenever there is a separation or slip between the two surfaces of the element, i.e., the displacement at point s on the positive surface is not equal to that of the corresponding point on the negative surface. The normal and shear displacement discontinuities, d_n and d_s, at the point s on the element axis are respectively defined as

$$d_n(s) = u_n(s, 0^-) - u_n(s, 0^+),$$

$$d_s(s) = u_s(s, 0^-) - u_s(s, 0^+),$$

where 0^- and 0^+ are respectively the n-coordinates of the negative and positive surfaces. In this case the fictitious quantities p_1 and p_2 are given by

$$p_1 = dd_s/ds; \quad p_2 = dd_n/ds.$$

If the distribution of the displacement discontinuity is constant, then

$$d_s(s) = D_b,$$

$$d_n(s) = D_d,$$

and we have a constant displacement discontinuity element. D_b and D_d are the fundamental variables. The induced stresses and displacements due to a constant displacement discontinuity element (CDDE) can be found by superposing two semi-infinite dislocations (Fig. 6). The dislocation at the end of the element is called a closure dislocation because it undoes the opening or closing of the dislocation at the beginning of the element (see Fig. 6). The closure dislocation is needed to model embedded fractures. For surface fractures the closure dislocation is not needed for the daylighting element and in this case a constant displacement discontinuity surface element (CDDSE) results.

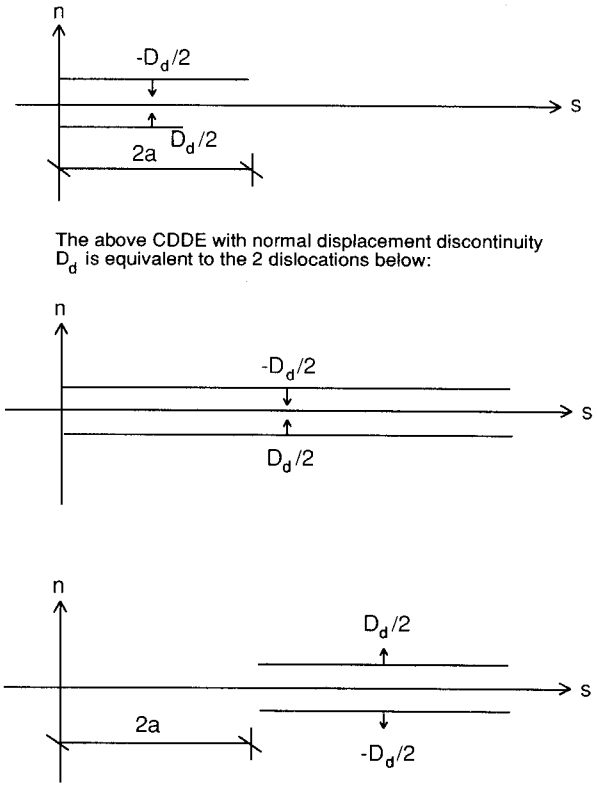

Fig. 6. Superposing 2 dislocations to form a CDDE.

When the displacement discontinuity is linearly distributed, i.e.,

$$d_s(s) = [1 - s/(2a)]D_a + s/(2a)D_b$$

and

$$d_n(s) = [1 - s/(2a)]D_c + s/(2a)D_d,$$

we have a linear displacement discontinuity element (LDDE). If the closure dislocation is absent, a linear displacement discontinuity surface element (LDDSE) results.

Under linear elastic fracture mechanics (LEFM) assumptions, the relative slip and separation near a crack tip is proportional to the square root of the distance r from the tip. Thus another type of element, called the root-r displacement discontinuity element (RRE), is constructed and we have (note that $s = r$ along the element axis)

$$d_s(s) = D_b[s/(2a)]^{1/2}$$

and

$$d_n(s) = D_d[s/(2a)]^{1/2}.$$

The stress intensity factors can then be conveniently calculated as

$$K_{\mathrm{I}} = KD_d$$

and

$$K_{\mathrm{II}} = KD_b,$$

where $K = \pi^{1/2}E/[8a^{1/2}(1 - \nu^2)]$ for plane-strain, and E and ν are respectively the Young's modulus and Poisson's ratio.

Another type of element, called the parabolic displacement discontinuity element (PDDE), has also been created with the following distributions of displacement discontinuity:

$$d_s(s) = D_b[s/(2a)]^2$$

and

$$d_n(s) = D_d[s/(2a)]^2.$$

The stresses at the tip of the PDDE are finite and hence it can be used to model tension-softening or slip-weakening processes at crack tips (in contrast to the RRE element where the stresses at the tip are infinite).

The influence functions of all the above types of displacement discontinuity elements have been derived in closed form by Chan [8].

2.2. Linear superposition and collocation

After the boundaries are discretized into a suitable element configuration, the fundamental variables associated with each of the elements, which can represent fictitious stresses or dislocations, are to be found. The first step is to calculate the induced stresses/displacements on the boundaries due to each of the fundamental variables using the corresponding influence functions. The resultant induced stresses/displacements at a boundary location due to all the fundamental variables can then be found by linear superposition, i.e., transforming the induced stresses/displacements using the local system of the particular location and adding them together.

The resultant induced stresses/displacements at a certain point (collocation point) on an element can then be equated to the imposed stresses or displacements and equations involving the unknown fundamental variables are established. The number of collocation equations must equal the number of unknown fundamental variables to result in a unique solution.

3. Deformation and fracture propagation modelling

3.1. A generalized representation of linear elastic boundary conditions

For an analysis step, the applied loading is regarded as a set of given boundary conditions. As mentioned in Section 2.2, the boundary conditions are enforced at the collocation points

Table 1. Constants expressing different boundary conditions

Boundary condition	Equation	Non-zero constants
Applied shear stress $\sigma_{sn}(M) = \tau^*$	(5)	$B(M, 1) = 1.0$, $B(m, 7) = \tau^*$
Applied normal stress $\sigma_{nn}(M) = \sigma^*$	(6)	$B(M, 9) = 1.0$, $B(M, 14) = \sigma^*$
Applied shear displacement $u_s(M) = h^*$	(5)	$B(M, 3) = 1.0$, $B(M, 7) = h^*$
Applied normal displacement $u_n(M) = v^*$	(6)	$B(M, 11) = 1.0$, $B(M, 14) = v^*$
Shear spring (Fig. 7a) $\sigma_{sn}(M) - k_s u_s(M) = 0.0$	(5)	$B(M, 1) = 1.0$, $B(M, 3) = -k_s$
Normal spring (Fig. 7b) $\sigma_{nn}(M) - k_n u_n(M) = 0.0$	(6)	$B(M, 9) = 1.0$, $B(M, 11) = -k_n$

of the elements. Let $\sigma_{sn}(M)$, $\sigma_{nn}(M)$, $u_s(M)$ and $u_n(M)$ be the stresses (in addition to initial stresses, if any) and displacements at a collocation point M of a certain element at the end of the step, then a generalized representation of the given boundary conditions is

$$B(M, 1) * \sigma_{sn}(M) + B(M, 2) * \sigma_{nn}(M) + B(M, 3) * u_s(M) + B(M, 4) * u_n(M) + B(M, 5) * DV_{M1} + B(M, 6) * DV_{M2} = B(M, 7) \ldots, \quad (5)$$

$$B(M, 8) * \sigma_{sn}(M) + B(M, 9) * \sigma_{nn}(M) + B(M, 10) * u_s(M) + B(M, 11) * u_n(M) + B(M, 12) * DV_{M1} + B(M, 13) * DV_{M2} = B(M, 14) \ldots \quad (6)$$

DV_{M1} is the change in the first fundamental variable at collocation point M during the step. Similarly DV_{M2} is the change in the second fundamental variable. For example, for a constant element such as a constant stress discontinuity element or constant displacement discontinuity element (CSDE or CDDE), DV_{M1} is the change in D_b and DV_{M2} is the change in D_d during the step.

$B(M, 1)$ to $B(M, 14)$ are a set of constants which dictate the boundary conditions at collocation point M. Table 1 lists different combinations of $B(M, 1)$ to $B(M, 14)$ which represents the applied stress, applied displacement, and spring boundary conditions. The deformation behaviour of fractures can also be represented by shear and normal springs inside the fracture (Fig. 7). For each of the boundary conditions in Table 1, the constants which are not listed are to take the value zero. See [8, 9, 10] for details.

3.2. Formulation of system equations

A given problem geometry is first discretized into N boundary elements (see Figs. 1 and 5). Each of the N elements may have one or two collocation points, depending on the element type. There are two fundamental variables associated with each collocation point. Sometimes certain fundamental variables are expected not to change during a particular step of the analysis. A common example is that if a fracture remains closed during the step, then

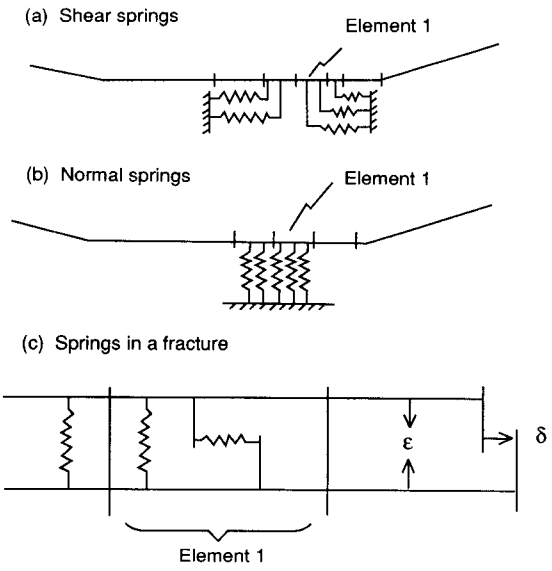

Fig. 7. Spring boundaries.

the normal fundamental variables (the normal displacement discontinuities) will remain zero. The fundamental variables which do not change during a step are inactive.

The system equations for a step are set up by considering the boundary conditions on the final stresses/displacements at the end of the step, (5) and (6), and the initial stresses/displacements at the collocation points associated with the active fundamental variables. Let $\sigma^0_{sn}(M)$, $\sigma^0_{nn}(M)$, $u^0_s(M)$ and $u^0_n(M)$ be the stresses/displacements at collocation point M at the beginning of the step. The changes from the initial to the final stresses are equal to the stresses induced by the active incremental fundamental variables [$\sigma^d_{sn}(M)$ and $\sigma^d_{nn}(M)$] and the stresses (if any) applied at infinity during the step [$\Delta\sigma^\infty_{sn}(M)$ and $\Delta\sigma^\infty_{nn}(M)$]:

$$\mathbf{x}_M = \mathbf{x}^d_M + \mathbf{x}^c_M \ldots, \tag{7}$$

where

$$\mathbf{x}_M = [\sigma_{sn}(M)\ \sigma_{nn}(M)\ u_s(M)\ u_n(M)]^T,$$

$$\mathbf{x}^d_M = \text{vector of induced stresses and displacements}$$

$$= [\sigma^d_{sn}(M)\ \sigma^d_{nn}(M)\ u^d_s(M)\ u^d_n(M)]^T,$$

$$\mathbf{x}^c_M = [\sigma^0_{sn}(M) + \Delta\sigma^\infty_{sn}(M)\ \sigma^0_{nn}(M) + \Delta\sigma^\infty_{nn}(M)\ u^0_s(M)\ u^0_n(M)]^T.$$

After expressing $\mathbf{x}^d_M$ in terms of the active fundamental variables through the corresponding influence functions (7) can be substituted into the boundary conditions (5) and (6). The resulting set of linear equations with the active fundamental variables as unknowns can then be solved.

In the above formulation the responses of the system are linear. However, nonlinear responses often occur due to the opening/closing, nonlinear stress-slip relations of the

fracture surfaces, and fracture propagation. To model nonlinear responses the given loading is applied in linear steps. This treatment of nonlinearities is discussed in the following sections.

3.3. Opening and closing of fractures

A fracture is modelled by a certain number of displacement discontinuity elements each of which may open or close due to the applied loading. Before any loadings are applied, all the fracture elements are assumed to be closed. If the applied loadings are compressive, the fracture will remain closed and the fundamental variables corresponding to the normal displacement discontinuities are de-activated. However, closed elements can still shear because the fundamental variables corresponding to the shear displacement discontinuities are still active. For example, in modelling the direct shear test on a rock joint, the normal fundamental variables of the joint (or fracture) elements are inactive while the shear fundamental variables are still active.

If the applied loadings cause opening displacements of a certain fracture element, as indicated by the solution of the system equations for the fundamental variables, the normal fundamental variables of that element will stay active. Thus the fracture opening can be modelled. However, if subsequent loadings cause the fracture element to close more than it has opened, its normal fundamental variables will be de-activated at the load level at which the element just closes. Any remaining or subsequent loadings will be applied with the normal fundamental variable of that element being inactive, unless tensile stresses occur across the fracture surfaces, indicating a re-opening of the fracture element.

3.4. Nonlinear stress-slip relations

For closed fracture surfaces the sliding behaviour can be modelled by nonlinear shear springs in the fracture (Fig. 7c) such that

$$\tau = \sigma f(\delta) + c \ldots, \tag{8}$$

where $f(\delta)$ represents the coefficient of friction, which is considered to be a multilinear function of δ. c is the cohesion constant.

$f(\delta)$ can be arbitrary and a typical form for fractures under high normal stresses is depicted in Fig. 8. Because of the dependence on σ, iterations are usually required to ensure that (8) is obeyed.

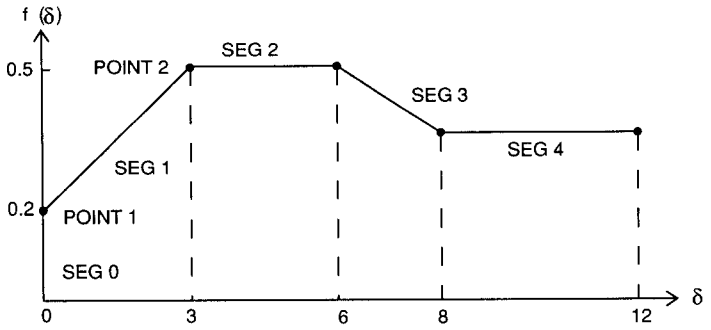

Fig. 8. Coefficient of friction as a function of slip.

3.5. Fracture propagation

As far as mixed-mode fracture propagation criteria are concerned, under the LEFM assumptions, three commonly known criteria are: (1) the maximum tensile stress factor [11], (2) the maximum energy release rate [12], and (3) the minimum strain-energy-density factor [13]. Based on a survey of experimental results [5, 8], for crack trajectory prediction, all the three methods have been found to be satisfactory while for critical load prediction there is no preferred choice. However, the maximum tensile stress factor has been found to be computationally most efficient and has thus been incorporated into the hybridized scheme.

Usually fracture tips are modelled by RRE's. For each RRE the stress intensity factors are calculated at the end of each attempted step and the maximum tensile stress factor criterion is used to check if propagation occurs. If propagation takes place, a new RRE is added in the direction of the maximum hoop stress. The old RRE is turned into an LDDE after propagation.

For a closed fracture, a slip-weakening constitutive law is employed and the stresses at the fracture tips can be evaluated. In this case the maximum tensile stress criterion, as described below, is used for determining fracture initiation and direction of the propagating crack. In the example shown in Fig. 9 the fracture is closed under compression and shear; the tips of the fracture are modelled by PDDE's (which have finite stresses at their tips, see Section 2.1.2) while the body of the fracture is usually modelled by LDDE's. Since the fracture is closed, shear spring boundary conditions can be imposed on the LDDE's and the 2 PDDE's. As the

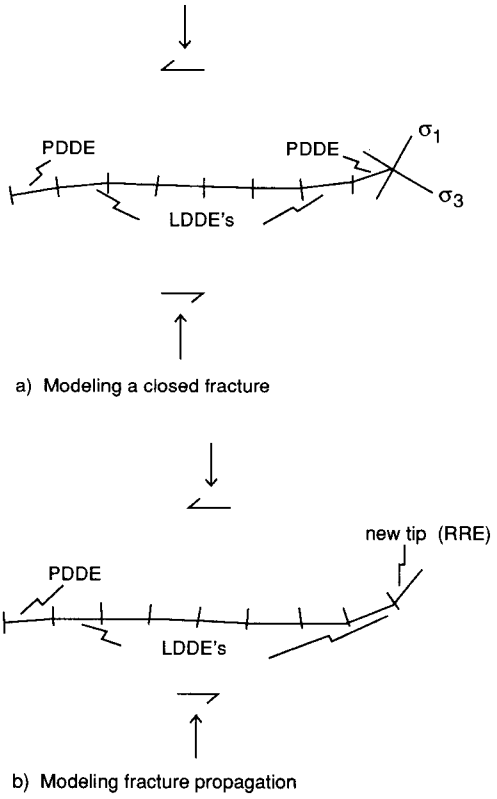

Fig. 9. Fracture propagation from a closed fracture.

analysis progresses with increasing applied load, the stresses at the tip of each PDDE are evaluated at the end of each step. When the magnitude of the maximum tensile stress at the tip, which is simply the minimum principal stress (compression is positive), reaches the tensile strength, the fracture propagates and a new RRE is added (Fig. 9b). The direction of the new RRE is perpendicular to the maximum tensile stress direction. LEFM assumptions are then used for the propagation of the newly created RRE.

4. Example applications

The concepts and formulations developed in the previous sections have been incorporated into the computer code FROCK. Various case studies have been performed to verify and test the capability of the program (see [8]). A few examples from these case studies are presented in the following sections. Consistent units are used in all the cases.

4.1. Rectangular plate under compression

This is the simple case of a rectangular plate under uniaxial compression. The geometry, material properties and loading conditions are shown in Fig. 10. Different types of elements are used to simulate the four sides of the plate so that their suitability in modelling finite

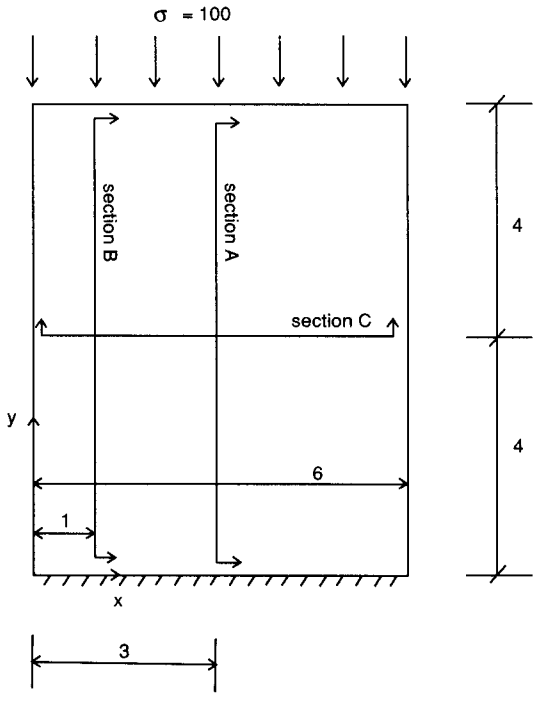

Fig. 10. Rectangular plate under compression.

boundaries can be compared. In each case, three elements are used to simulate a horizontal side and four for a vertical side.

CDDE's, LDDE's, CSDE's, and LSDE's are used in four separate cases and the calculated stresses and displacements using FROCK along the mid-sections (A and C) are derived. Generally, the calculated results compare satisfactorily with the simplified analytical solutions assuming a constant state of strain. Exceptions occur at points near the edges of the plate where the singularities at the ends of the elements have a considerable effect on the results. Accuracy generally increases from CDDE, to LDDE, to CSDE, and to LSDE. For example, the average u_y along Section C calculated using LSDE's differs by 2 percent from the simplified analytical solution. The corresponding relative errors using CSDE's, LDDE's and CDDE's are respectively 2%, 7% and 9%.

On sections near the edges (and hence nearer to the elements) the singularities at the ends of the elements cause the calculated results to fluctuate. The most noticeable fluctuations occur when using CDDE's. For example, in Section B, σ_y varies in a wavy manner between 100 and 123 with a mean at about 106. The fluctuations are smaller with LDDE's and are still less with CSDE's. With LSDE's σ_y stays fairly constant at about 100, the correct value, except near the bottom. Thus the stress discontinuity elements can better model the plate boundaries than the displacement discontinuity elements due to their smaller singularities.

4.2. Stress intensity factors

4.2.1. Single crack

Stress intensity factors (SIF's) are calculated in two different ways: (1) based on the standard analytical expressions for LEFM crack tip opening and sliding displacements, and (2) using the computed displacement discontinuities (Section 2.1.2). The SIF's of a straight crack with internally applied pressure and shear tractions applied at infinity (see Fig. 11) are compared. Figure 11 also lists the analytically derived K_I and K_{II}. The crack tips are modelled by RRE's and the crack body by LDDE's. The effect of element configuration (number of elements and their relative size) on the accuracy of the SIF's calculated by FROCK are examined. Between 2 and 50 elements were used to model the crack. If all the elements have the same size, then the calculated SIF's are accurate to within 5 percent of the theoretical values, except for extreme cases, such as those where only two or three elements were used, where errors of 21% and 10% respectively occurred.

In the above test cases, the collocation points of the RRE's and LDDE's are located as shown in Fig. 12. Case studies (see [8]) indicate that varying the locations of the collocation points of the LDDE's (with k varying between 0.1 and 2/3) did not appreciably change the calculated SIF's. The locations of the collocation points of the RRE's however are much more important and, generally, the results are satisfactory for $1.0 < k < 1.8$.

4.2.2. Two aligned cracks under tension and shear (Fig. 13)

In Table 2 the SIF's at tips A and B as obtained analytically [14] are compared with the results from FROCK. The amplification of the SIF's due to crack interaction is shown by also listing the (analytical) SIF's of the single crack case. Two crack configurations with different x_1 and x_2 (see Fig. 13) have been used.

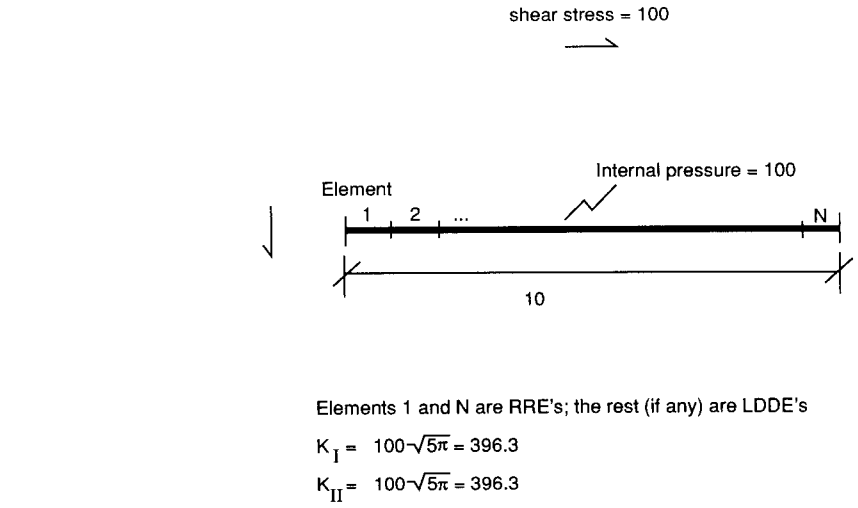

Fig. 11. Single crack with internal pressure and shear at infinity.

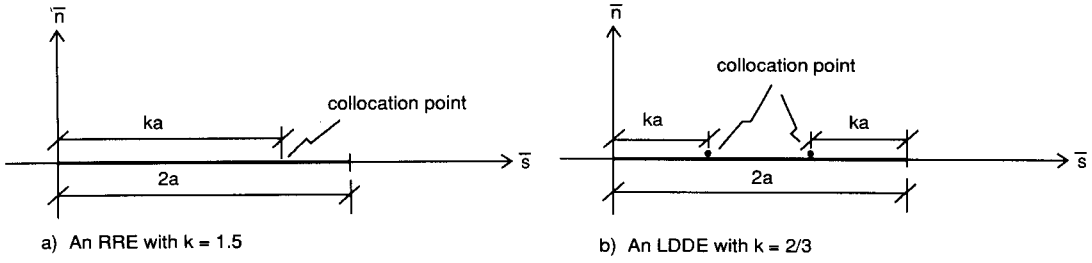

Fig. 12. Location of collocation points.

Table 2. SIF's of two aligned cracks

	Crack geometry 1: $x_1 = 10$, $x_2 = 20$ (see Fig. 13)		Crack geometry 2: $x_1 = 0.87156$, $x_2 = 10$ (see Fig. 13)	
	SIF at Tip A:	SIF at Tip B:	SIF at Tip A:	SIF at Tip B:
$K_{I(\text{one crack only})}$	396	396	379	379
$K_{I(\text{FROCK})}$	403	401	470	418
K_I [14]	403	401	490	414
$\frac{K_{I(\text{FROCK})}}{K_I\ [14]}$	1.00	1.00	0.96	1.01
$K_{II(1\text{ crack})}$	198	198	189	189
$K_{II(\text{FROCK})}$	202	201	235	209
K_{II} [14]	202	201	245	207
$\frac{K_{II(\text{FROCK})}}{K_{II}\ [14]}$	1.00	1.00	0.96	1.01

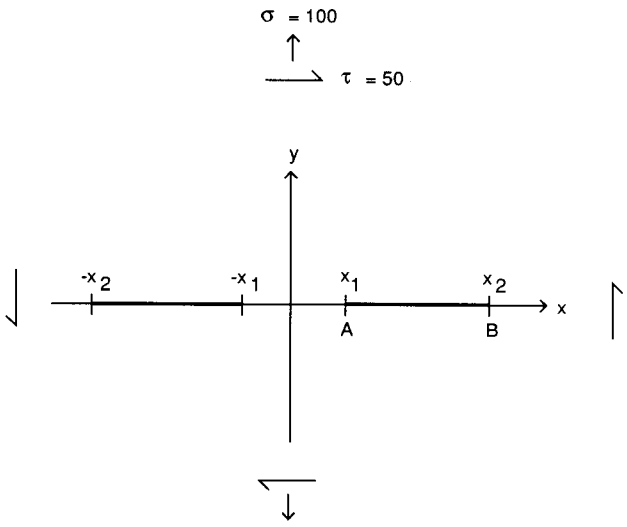

Fig. 13. Two aligned cracks under tension and shear.

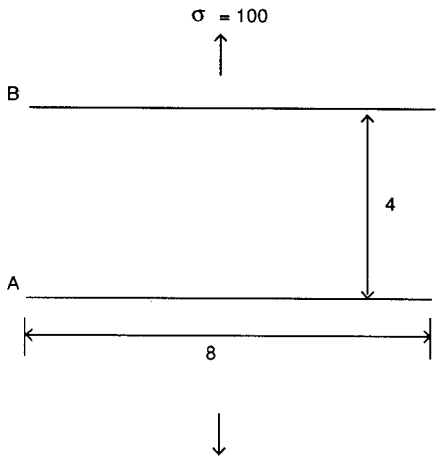

Fig. 14. Two equal parallel cracks.

Table 3. SIF's of two equal parallel cracks (at tip A)

	Number of elements: (N = 8)	Number of elements: (N = 20)
	SIF at A:	SIF at A:
$K_{I(FROCK)}$	254.2	272.7
K_I [15]	268.3	268.3
$K_{I(FROCK)}/K_I$ [15]	0.95	1.02
$K_{II(FROCK)}$	−38.03	−41.78
K_{II} [15]	−43.18	−43.18
$K_{II(FROCK)}/K_{II}$ [15]	0.91	0.97
$K_{I(one\ crack\ only)}$	354.5	354.5
$K_{II(one\ crack\ only)}$	0.0	0.0

4.2.3. Two parallel cracks of equal width under tension (Fig. 14)

In Table 3 the SIF's at tip A calculated using FROCK are compared with the results obtained by Yokobori et al. [15], who used a numerical procedure to derive his results. Two cases with different numbers of elements (8 and 20) were investigated. Since the cracks have the same length in both cases, the size of the elements is smaller in the second case. It can be seen that, in the latter case, the FROCK results are closer to Yokobori's results. Thus for strong interactions of cracks more elements are needed. Strong interactions are considered to occur, if the SIF's of the two interacting cracks deviate considerably from the SIF of the case with only one crack (for this reason the SIF's of a single crack are also given in Table 4).

4.2.4. Two equal stepping cracks under tension (Fig. 15)

The SIF's at tips A and B calculated with FROCK are compared with the results by Yokobori et al. [15], who again used a numerical procedure to arrive at their results. Two configurations having the same crack sizes but different numbers of elements (8 and 20) are examined; in addition, 4 different values of T (see Fig. 15), ranging from 0.5 to −0.25, are used. The FROCK results are within 2 percent of Yokobori's values for K_I at A and usually

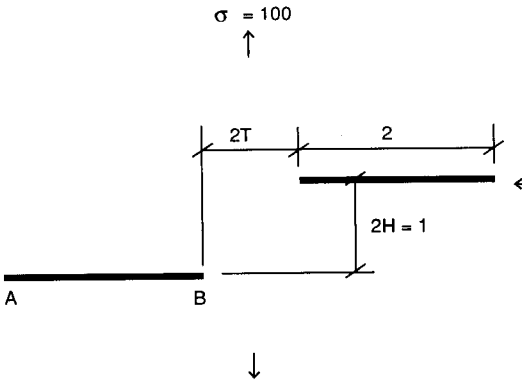

Fig. 15. Two equal stepping cracks.

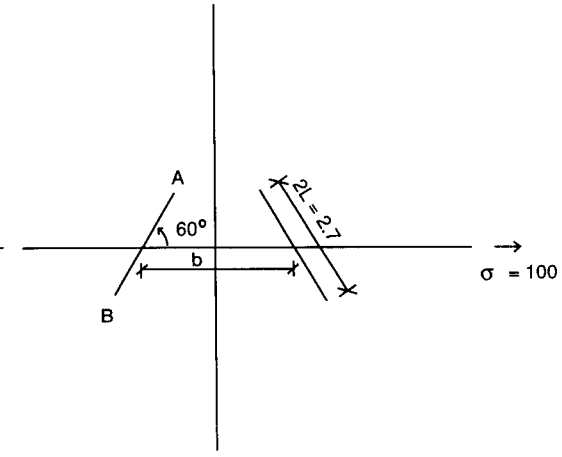

Fig. 16. Two inclined cracks under tension.

Table 4. SIF's of two inclined cracks

	Crack geometry Distance b (see Fig. 16)	
	6.0	3.0
	SIF:	SIF:
K_{IAI}	144	123
K_{IAF}	144	121
K_{IAF}/K_{IAI}	1.00	0.98
K_{IIAF}	−85	−80
K_{IBI}	149	140
K_{IBF}	147	137
K_{IBF}/K_{IBI}	0.99	0.98
K_{IIBF}	−83	−73

within 5 percent for K_{II} at A and K_I at B. In general, if more and thus smaller elements are used, the results are closer to those by Yokobori et al. [15]. For K_{II} at B, deviations between 1 and 50 percent occur with the difference increasing as the distance T between the two crack tips increases. At present, we have no idea what causes these discrepancies.

4.2.5. Two inclined cracks of equal width under tension (Fig. 16)
In Table 4 the SIF's at tips A and B calculated with FROCK (K_{IAF}, K_{IBF}) are compared with the results obtained by Isida [16] using a numerical approach (K_{IAI} and K_{IBI} only, K_{II} were not calculated by Isida). Two cases with different values of b are examined. Although only 8 elements are used for each crack, the results compare very well in each case because, as stated by Isida, "the enclosing circles of all the cracks are not so close to each other", i.e., the cracks are not so close as to interact strongly.

5. Conclusions

A general-purpose numerical procedure (FROCK) based on the displacement discontinuity and indirect boundary element methods has been developed. The procedure has been applied

to various two-dimensional problems with or without existing fractures and the results usually compare satisfactorily with existing solutions. Future papers will address more complex case studies and engineering applications. The strong points of the procedure as compared to most other existing methods are:

(i) Analytic influence functions of the boundary elements have been derived, and thus numerical integration is not required. This means that the only source of inaccuracy (apart from computer roundoff errors) is from the approximation of the boundary conditions by collocation. Also only single precision variables are required in the computation of the influence functions.

(ii) External boundaries and fractures of arbitrary geometries can be conveniently modelled. Fracture propagation is automatically modelled by FROCK, and there is no need to substructure (or partition) the medium. No re-meshing is required. Both finite and infinite media are possible.

(iii) Closed fracture (or parts of fractures) are realistically modelled by non-linear shear stress-slip relations, which depend also on the normal stress. For closed fracture tips, a slip-weakening law is implemented and the stresses at the tips can be calculated.

(iv) Arbitrary loading sequences are possible. The modelled fractures (or parts of them) can open or close in response to the applied loadings. The problem status after each stage of loading can be stored and recalled later for further analysis.

(v) Geostatic stresses can be included in the analysis so that in-situ conditions are modelled more realistically.

Acknowledgements

Research which led to the development of "A Hybridized Displacement Discontinuity and Indirect Boundary Element Method to Model Fracture Propagation" and the associated computer program FROCK has been sponsored by the U.S. Army Research Office under grant No. DAAG24-83-K-0016. This support and the interest of the technical project monitor, Dr. S. Mock is greatly appreciated.

References

1. K.J. Bathe, *Finite Element Procedures in Engineering Analysis*, Prentice-Hall, New Jersey (1982).
2. S.L. Crouch and A.M. Starfield, *Boundary Element Method in Solid Mechanics*, G. Allen & Unwin Publ. Ltd. (1983).
3. J.H. Curran and L. Vadamme, "Determination of the two-dimensional distribution of stress around a crack", University of Toronto Publication 83–10 (1983).
4. C.A. Brebbia, J.C.F. Telles and L.C. Wrobel, *Boundary Element Techniques*, Springer-Verlag, NY (1984).
5. A.R. Ingraffea, *Rock Fracture Mechanics*, Springer-Verlag, NY (1983).
6. G. Blandford et al., *International Journal for Numerical Methods in Engineering* 17 (1981) 387–404.
7. S.P. Timoshenko and J.N. Goodier, *Theory of Elasticity*, 3rd edn., McGraw-Hill, NY (1970).
8. H.C. Chan, "Automatic Two-dimensional Multi-fracture Propagation Modelling of Brittle Solids with Particular Application to Rock", Sc.D dissertation, Massachusetts Institute of Technology (1986).
9. N. Fares and V.C. Li, *Engineering Fracture Mechanics* 26 (1987) 127–141.
10. W.J. Roberds, "Numerical Modelling of Jointed Rock", Ph.D. thesis, Massachusetts Institute of Technology (1979).

11. F. Erdogan and G.C. Sih, *Journal of Basic Engineering* 85 (1963) 527.
12. M.A. Hussein, S.L. Pu and J. Underwood, in *Fracture Analysis, ASTM STP 560* (1974) 2–28.
13. G.C. Sih, *International Journal of Fracture* 10 (1974) 305–321.
14. H. Tada, P.C. Paris and G.R. Irwin, *The Stress Analysis of Cracks Handbook*, Del Research Corp, Hellertown, PA (1973).
15. T. Yokobori, M. Uozumi and M. Ichikawa, *Report of the Institute of Strength and Fracture of Materials* 7 (1971) 25–47.
16. M. Ishida, *Bulletin of the Japan Society of Mechanical Engineers* 13 (1970) 59.